POLITECNICO DI TORINO
Repository ISTITUZIONALE

A New Steklov-Poincare Numerical Technique for Solving Prandtl-Batchelor Flows

(Article begins on next page)

24 April 2024

A new Steklov-Poincaré numerical technique for solving Prandtl-Batchelor flows

Michele Ferlauto, and Luca Zannetti

A New Steklov-Poincaré Numerical Technique for Solving Prandtl-Batchelor Flows

Michele Ferlauto[1,a),b)] and Luca Zannetti[2]

[1]*Department of Mechanical and Aerospace Engineering, Politecnico di Torino, Turin, Italy*
[2]*Accademia delle Scienze di Torino, Turin, Italy*

[a)]Corresponding author: michele.ferlauto@polito.it
[b)]URL: http://staff.polito.it/michele.ferlauto

Abstract. The Prandtl-Batchelor flow model is a well-known asymptotic solution of the Navier-Stokes equations often used as a paradigm model of wake past bluff bodies. The main concern is the derivation of vortex equilibria and stability in symmetric and asymmetric configurations. The numerical solution of such class of problems requires an high resolution of the flow in the wake regions and a wide grid to accurately match asymptotic conditions at infinity. In this work a numerical technique based on the Steklov-Poincaré iterative scheme is proposed in order to match the asymptotic conditions and a high resolution on the wake. The case of body endowed with sharp edges is also considered.

INTRODUCTION

Vortex models of wakes past bluff bodies are of great interest in a wide range of engineering applications [1, 2, 3, 4]. In the present work we focus on the steady configuration of two-dimensional flows past bluff bodies at Reynolds number Re $\rightarrow \infty$ discussed by Batchelor [5]. These asymptotic solutions of the Navier-Stokes equations, generally designated as "Prandtl-Batchelor flows", are peculiar solutions among the infinity admitted by the Euler equations. The flow is thought as uniform at infinity and irrotational except inside the finite area wake past the bluff body. The wake is formed by vortex patches of vorticity and bounded by vortex sheets and/or closed streamlines. Fundamental problems of vortex dynamics [6, 3] as well as recent technologies for high-lift or low-drag devices[1, 2] rely on such flows. The existence of vortex equilibria are of interest even in case of unstable configurations. In fact, stability can be augmented artificially by active flow control [7]. From the numerical perspective, the accurate assessmemnt of the vortex equilibria is challenging. A fine grid is required in order to accurately resolve the vortex regions, whereas the computational domain should be large enough to replicate the boundary conditions at infinity. A straightforward application of any standard solution method to the problem in the entire domain would require a very large number of grid points[3]. In present paper conformal mapping techniques, domain decomposition and asymptotic expansions of the boundary conditions are combined together to overcome the technical difficulties mentioned above. The resulting scheme belongs to the class of the Steklov-Poincaré approaches.

MATHEMATICAL MODEL

The Prandtl-Batchelor flows are solutions of the steady 2-D Euler equations. By expressing the velocity $\mathbf{u}$ in terms of the stream-function ψ as $\mathbf{u} = [u, v]$, with $u = \partial\psi/\partial y$ and $v = -\partial\psi/\partial x$, we are lead to the boundary value problem

$$\begin{cases} \nabla^2\psi = F(\psi) & \text{in } \Omega \\ \psi = \psi_b & \text{in } \partial\Omega \end{cases} \tag{1}$$

where $F(\psi)$ is an a priori undefined function and the function ψ_b depends on the boundary conditions on the normal velocity component $u_N = \mathbf{u} \cdot \mathbf{n}$, being $\mathbf{n}$ the unit normal vector facing out of the domain Ω. Portions of the boundary

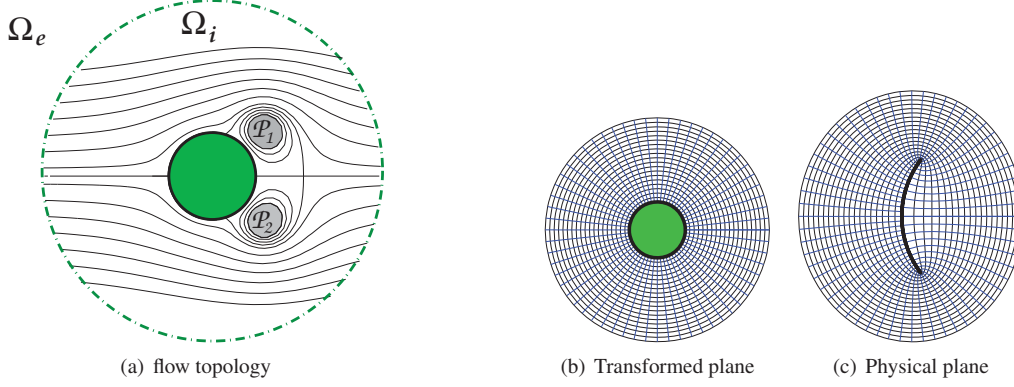(a) flow topology (b) Transformed plane (c) Physical plane

FIGURE 1. topological sketch of the flow (a) and example of corresponding grids on the map working planes (b,c).

$\partial\Omega$ where the $u_N = 0$ are streamlines, because ψ_b reduces to a constant. On the parts of the boundary where $u_N \neq 0$, as for instance in a inflow or outflow boundary, ψ_b is obtained by integration of $(\partial\psi/\partial s)_b = u_N$ along the curvilinear coordinate s on $\partial\Omega$. As described in Gallizio et al.[3], under certain assumptions the entire steady flow field past a bluff body can be modelled as the coupling of an irrotational region exterior to the wake, and the wake represented by patches of constant vorticity ω. Assuming symmetric/asymmetric wake configurations represented by two vortex patches, the vorticity field is expressed in the right-hand side of Eq.(1) as

$$F(\psi) = \omega_1 g(\psi - \alpha_1) + \omega_2 g(\psi - \alpha_2), \qquad g(\psi, \alpha_j) = H[\, sgn(\alpha_j) * (\psi - \alpha_j)] \tag{2}$$

where $H()$ denotes the Heaviside function, ω_1, ω_2 are (constant) vorticity values, and α_1, α_2 are the values of the stream-function ψ on the boundary $\partial\mathcal{P}_j$ of each vortex patch $\mathcal{P}_j$. It must be stressed that the shapes of the vortex patches P_j are not a priori determined and must be found as a part of the solution of the problem. Under these assumptions, an explicit form of the free-boundary problem (1) is given by

$$\nabla^2\psi_1 = \omega_1 \quad \text{in } \mathcal{P}_1; \qquad \nabla^2\psi_2 = \omega_2 \quad \text{in } \mathcal{P}_2; \qquad \nabla^2\psi_3 = 0 \quad \text{in } \Omega\backslash(\mathcal{P}_1 \cup \mathcal{P}_2); \tag{3}$$

$$\psi_1 = \psi_3 = \alpha_1, \quad \frac{\partial\psi_1}{\partial n} = \frac{\partial\psi_3}{\partial n} \quad \text{on } \partial\mathcal{P}_1; \qquad \psi_2 = \psi_3 = \alpha_2, \quad \frac{\partial\psi_2}{\partial n} = \frac{\partial\psi_3}{\partial n} \quad \text{on } \partial\mathcal{P}_2; \qquad \psi_3 = \psi_b \quad \text{on } \partial\Omega. \tag{4}$$

The functions ψ_1, ψ_2, ψ_3 are the restrictions of the stream-function ψ with respect to the vortex patches $\mathcal{P}_1, \mathcal{P}_2$, and to the complement of their union in Ω.

NUMERICAL METHOD

The physical domain is mapped into a suitable transformed plane ζ, e.g. a circle, by conformal mapping. As visible in Figure 1, on the latter the domain is decomposed into two subdomains: (i) a small interior subdomain Ω_i which includes the image of the recirculating flow, and (ii) an exterior subdomain Ω_e comprising the remainder of the flow field which extends to infinity. The streamline $\psi = \alpha_j$, which separates each rotational region $\mathcal{P}(\alpha_j)$ from the surrounding irrotational domain $\Omega_i\backslash\mathcal{P}(\alpha)$, is detected as a jump of the vorticity ω_j represented on the grid. System (4) is solved numerically by combining a finite-difference approach in the interior subdomain Ω_i with an analytical expression for the solution of the Laplace equation in the exterior subdomain Ω_e. The two solutions are coupled through the boundary conditions on the interface $r = \rho$ separating the two subdomains: for the interior problem we use the Dirichlet boundary condition $\psi_i = \psi_e$, whereas for the exterior subproblem the Neumann boundary condition $\partial\psi_e/\partial n = \partial\psi_i/\partial n$. The subscripts 'i' and 'e' refer to the solutions defined on the interior and the exterior subdomains. Repeated solution of such two coupled problems in known as the Steklov-Poincaré iteration which is a well-known approach in the domain decomposition literature [8]. According to the Riemann mapping theorem [9, 10], any arbitrary simply-connected region can be conformally mapped onto a circle interior/exterior. System (4) is transformed to the

ζ-plane with $\zeta = \xi + i\eta$ acting as the independent variable. By defining the operator $\nabla_\zeta^2 = \partial_\xi^2 + \partial_\eta^2$, we have

$$\nabla_\zeta^2 \psi = \frac{1}{J} \sum_{j=1}^{2} \omega_j H(\psi - \alpha_j), \qquad \text{with} \quad J = |dz/d\zeta|^{-2} \tag{5}$$

The interior subdomain Ω_i coincides with the annulus region within $1 \leq r \leq \rho$ of Figure 1a. In the interior subdomain Ω_i the boundary conditions $\psi_i(1) = 0$ and $\psi_i(\rho) = \psi_b$ are imposed. The latter Dirichlet boundary condition is expressed in terms of the solution ψ_e in the exterior subdomain Ω_e. The proposed method is based on the Schauder fixed point theorem [11]. Accurate far-field conditions have been imposed by using a modification of the one-shot approach of Wang [12]. Let the stream-function ψ_i be defined by

$$\psi_i(\zeta) = \psi_0(\zeta) + \omega_1 \psi_1(\zeta) + \omega_2 \psi_2(\zeta) + \psi_3(\zeta) \qquad \text{in } \Omega_i \tag{6}$$

where the function ψ_0 satisfies the system with a homogeneous RHS and inhomogeneous boundary conditions,

$$\begin{cases} \nabla_\zeta^2 \psi_0 = 0 & \text{in } \Omega_i \\ \psi^0 = 0 & \text{at } r = 1 \\ \psi^0 = \psi_b & \text{at } r = \rho \end{cases} \tag{7}$$

whereas the functions ψ_1, ψ_2 satisfy the systems

$$\begin{cases} \nabla_\zeta^2 \psi_1 = J^{-1} & \text{in } \mathcal{P}_1 \\ \nabla_\zeta^2 \psi_1 = 0 & \text{elsewhere} \\ \psi_1 = 0 & \text{at } r = \rho \end{cases} \qquad \begin{cases} \nabla_\zeta^2 \psi_2 = J^{-1} & \text{in } \mathcal{P}_2 \\ \nabla_\zeta^2 \psi_2 = 0 & \text{elsewhere} \\ \psi_2 = 0 & \text{at } r = \rho \end{cases} \tag{8}$$

characterized by inhomogeneous RHS and homogeneous boundary conditions.

Far-field boundary conditions.

The far-field boundary condition here adopted is based on a non-iterative strategy suggested by Wang [12]. With reference to Figure 1a, inside Ω_i, that is for $1 \leq r \leq \rho$), the stream-function is defined as $\psi = \Psi_i = \tilde{\psi} + \psi_d$. $\tilde{\psi}$ is based on the flow structure inside Ω_i. By comparison with eqs.(6-8), it is $\tilde{\psi} = \psi^0 + \omega_1 \psi_1 + \omega_2 \psi_2$. the function ψ_d is a post-correction function that ensures the enforcement of boundary condition at infinity. Similarly, in the exterior domain Ω_e ($r > \rho$) we set $\psi = \Psi_e$. On the circle in the transformed plane, at $r = 1$, is

$$\Psi_i(1) = 0, \qquad \tilde{\psi}(1) = 0, \qquad \psi_d(1) = 0 \tag{9}$$

At the boundary $\partial\Omega_i$, for $r = \rho$, we impose

$$\Psi_i(\rho) = \Psi_e(\rho), \qquad \frac{\partial \Psi_i}{\partial r}(\rho) = \frac{\partial \Psi_e}{\partial r}(\rho) \tag{10}$$

After expressing the functional form of ψ_d by a Laurent series and adding a similar contribution on Ψ_e, the coefficients of the unknown series can be deduced by the relations (9)-(10) according to the procedure presented in Ref. [12].

Enforcement of the Kutta condition.

The most studied examples of Prandtl-Batchelor flows represent vortex equilibria past bodies with or without geometric discontinuities as sharp edges or cusps [13]. In inviscid models, the regularity condition for such flows at the geometric discontinuity is expressed by the Kutta condition. In the example of Figure 2 there are two separation points corresponding to the arc edges A and B. The enforcement of Kutta conditions at points ζ_A, ζ_B removes the flow singularities and allows us to compute the vorticity levels ω_1, ω_2 of vortex patches.

$$\left. \frac{\partial \psi}{\partial r} \right|_{\zeta_A} = 0, \qquad \left. \frac{\partial \psi}{\partial r} \right|_{\zeta_B} = 0 \tag{11}$$

Finally we can resume the proposed algorithm is composed of the following steps: (i) compute ψ^0, ψ_1 and ψ_2 by solving the Poisson systems (7)-(8) separately; (ii) compute the correction function ψ_d for a closer matching of the far-field BCs; (iii) impose the Kutta conditions and derive the new vorticity levels ω_1, ω_2; (iv) compute the ψ-residuals; (v) iterate to point (i) until convergence .
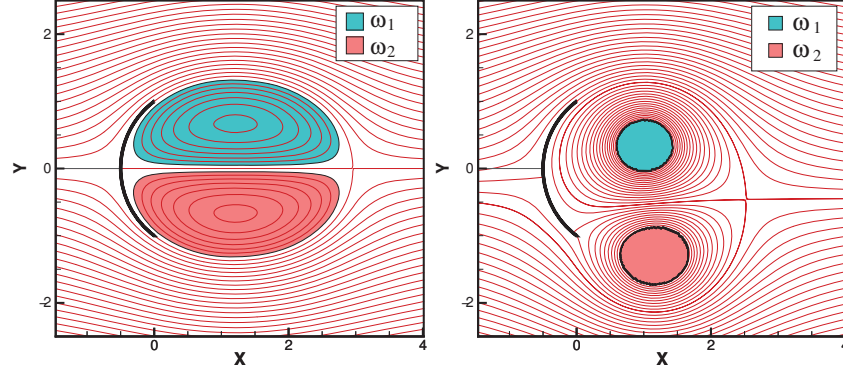
FIGURE 2. Steady vortex patch configurations: (a) symmetric and (b) asymmetric case .

NUMERICAL RESULTS

As an example of Prandtl-Batchelor flow, the equilibrium of two vortex patches behind an arc is investigated. The interested reader can find motivations, description of the flow and the point-vortex solutions of symmetric and asymmetric equilibrium configurations in Ref. [13]. By the proposed procedure we solve the more complex task of finding shape, positions and strength of two vortex patches instead of point vortices. The mapping function is $z = [a\zeta + b - 1/(a\zeta + b)]/2$, with $a = |i - b|$. For reference values α_1, α_2 that enclose patches of very small area, the point-vortex solution is found with high accuracy. The symmetric solution of with two large vortex of constant vorticity is shown in Figure 2(a). The reference value are $\alpha_1 = -\alpha_2 = -0.1$. The total circulation of null.

It is less intuitive that also steady asymmetric configurations with zero net circulation can be found [13]. The asymmetric configuration for the case with $\alpha_1 = -1.9$, $\alpha_2 = 0.94$ is shown in Figure 2(b). In both computations a grid of 2048×2048 has been used. The convergence to a solution for any combination of α_1, α_2 is not ensured. The first attempt configuration is therefore deduced from the knowledge of the point-vortex solution, which is a fair approximation of the vortex-patches centroids.

CONCLUSIONS

A numerical technique based on a new Steklov-Poincaré iterative scheme is proposed. It is able to match the accurate asymptotic conditions at infinity with the high resolution of vortex regions in the computation of vortex dominated flows according to the Prandtl-Batchelor model. Bluff bodies are replicated by conformal mapping. The technique is employed here for investigating steady vortex equilibria past a circular arc. Steady symmetric as well as asymmetric configurations of the vortex patches are obtained. The location, shapes and strengths of the vortex patches was part of solution of the problem.

REFERENCES

[1]   R. Rathnasingham and K. S. Breuer, J. Fluid Mech. **495**, 209–233 (2003).
[2]   M. Ferlauto and R. Marsilio, Advances in Aircraft and Spacecraft Science **2**, 77–94 (2014).
[3]   F. Gallizio, A. Iollo, and B. Protas, Physica D **239**, 190–201 (2010).
[4]   M. Ferlauto and S. Rosa Taddei, Proc. IMEchE Part A: Journal of Power and Energy **229**, 359–366 (2015).
[5]   G. K. Batchelor, J. Fluid Mech. **1**, 388–398 (1956).
[6]   S. I. Chernyshenko, Appl. Mech. Rev. **51**, 523–536 (1998).
[7]   B. Protas, Phys. Fluids **16**, 4473–4488 (2004).
[8]   A. Qarteroni and A. Valli, *Domain decomposition methods for PDEs* (Oxford University Press, 1999).
[9]   L. Zannetti, M. Ferlauto, and S. Llewellyn Smith, Journal of Fluid Mechanics **809**, 705–715 (2016).
[10] G. Carrier, M. Krook, and C. Pearson, *Functions of a complex variable* (SIAM, 2003).
[11] L. Gasinski and N. Papageorgiou, *Nonlinear Analysis* (Chapman & Hall, 2006).
[12] Z. J. Wang, Journal of Computational Physics **153**, 666–670 (1999).
[13] A. Elcrat, M. Ferlauto, and L. Zannetti, Fluid Dynamics Research **46**, 031407– (2014).